Article

Barrier Properties of Polylactic Acid in Cellulose Based Packages Using Montmorillonite as Filler

Daniela Sánchez Aldana [1], Eduardo Duarte Villa [2], Miguel De Dios Hernández [2], Guillermo González Sánchez [3], Quintín Rascón Cruz [1], Sergio Flores Gallardo [3], Hilda Piñon Castillo [3] and Lourdes Ballinas Casarrubias [1,*]

[1] Ciencias Químicas, Universidad Autónoma de Chihuahua, Circuito Universitario s/n, Campus Universitario No. 2, C.P. 31125, Chihuahua, Chih., Mexico; E-Mails: danielasav@hotmail.com (D.S.A); qrascon@uach.mx (Q.R.C.)

[2] Grupo COPAMEX, Ave. de la Juventud No. 280, C.P. 66450, San Nicolás de los Garza, N.L., Mexico; E-Mails: eduardo.duarte@copamex.com (E.D.V.); miguel.dedios@copamex.com (M.D.D.H.)

[3] Centro de Investigación en Materiales Avanzados, S.C., Laboratorio Nacional de Nanotecnología, Miguel de Cervantes No. 120, C.P. 31109, Chihuahua, Chih., Mexico; E-Mails: guillermo.gonzalez@cimav.edu.mx (G.G.S.); sergio.flores@cimav.edu.mx (S.F.G); hilda.pinon@cimav.edu.mx (H.P.C.)

* Author to whom correspondence should be addressed; E-Mail: lourdes.ballinas@gmail.com; Tel. +52-614-236-6000 (ext. 4288).

Abstract: Polylactic acid (PLA) and montmorillonite (CB) as filler were studied as coatings for cellulose based packages. Amorphous (AM) and semi crystalline (SC) PLA were used at different concentrations according to a $2 \times 6 \times 3$ full factorial experimental design. CB loading was three concentrations and coating was performed by casting. Contact angle (CA), water vapor (WVP) and grease permeabilities were measured for each resultant package and were compared to commercial materials (Glassine Paper, Grease Proof Papers 1 and 2 produced commercially). Significant differences were found and the main factors were the type and concentration of PLA. The best values were: for grease penetration, +1800 s; WVP from 161.36 to 237.8 $g \cdot \mu m \cdot kPa^{-1} \cdot m^{-2} \cdot d^{-1}$ and CA from 69° to 73° for PLA–AM 0.5% and CB variable. These parameters are comparable to commercial packages used in the food industry. DSC revealed three different thermal events for PLA–SC and just T_g for PLA–AM. Crystallinity was also verified, obtaining a ΔH_{crys} of 3.7 $J \cdot g^{-1}$ for PLA–SC and 14 $J \cdot g^{-1}$ for PLA–SC–BC, evidencing clay interaction as a

crystal nucleating agent. Differences found were explained on terms of the properties measured, where structural and chemical arrays of the coatings play a fundamental role for the barrier properties.

Keywords: polylactic acid; grease barrier; water vapor permeability; cellulose; montmorillonite

---

1. Introduction

Cellulose is the main material employed for food packaging due to its high availability, biodegradability and low cost. Nevertheless, these cellulose based packages usually present poor grease resistance, water vapor permeability and gas barrier capacities. For these reasons cellulose fiber paper should be coated with polymers that enhance these properties for food preservation. Many of the polymers employed to improve barrier properties are synthetic polymers that are toxic if ingested and non-biodegradable. Furthermore, in some cases, these chemical compounds could migrate into foodstuff and can be orally consumed. Commonly, food packaging industry has employed fluorocarbon chemical treatment to inhibit the wetting of cellulose fibers by reducing the surface energy of the sheet [1]. Perfluoro compounds have been recognized as materials with unique properties of stability and resistance to degradation [2]. In addition, fluorinated hydrocarbon has been used to provide grease resistance for paperboard products [3]. Begley *et al.* [2] determinated the perflourochemicals presented in food packaging and cookware as well as the migration potential of these compounds into foods oil.

The food packaging industry is seeking to replace the fluorinated synthetic polymers with natural and biodegradable materials which present grease, water vapor and gas barrier properties. For this reason, various natural biodegradable polymers including proteins, lipids and polysaccharide-based coatings have been proven such as zein [4,5], chitosan-beeswax [6], chitosan [7,8] and hydroxy-propyl methylcellulose [9]. However, many of them are partially hydrophilic resulting in a reduction of their barrier properties at high humidity [10].

Polylactic acid (PLA) is a compostable and renewable biopolymer produced from lactic acid derived from the corn, sugar cane or potato fermentation process [11] which has been commercialized as a great alternative which substitutes synthetic polymers [12]. Corn starch fermentation provides an abundant supply of lactic acid and its polymerization into polylactic acid produce a thermoplastic bio-polyester with properties comparable to petroleum polymers [13]. In addition, PLA properties could be modified by the ratio between the two lactic acid molecules (D-lactide and L-lactide) which composed it, ranging from an amorphous to a semi or highly crystalline material [14].

PLA is one of the biopolymers with most potential for plastic industries, because of its high mechanical properties, low hydrophobicity, low cost and processability compared to other alternatives. These characteristics makes it popular for a variety of applications like in food packaging [15,16] and into the medical field [17]. PLA has been used as an alternative to synthetic materials with good mechanical and tensile properties [17–22] which presents low oxygen permeability [15]; however, to the best of our knowledge, barrier properties to grease and water over a cellulose substrate are unexplored yet. Although the manufacturer's specifications recognized that PLA is a good barrier

agent to fat or oil, there are no studies in which the effect of food grease is evaluated. Moreover, many reports are focused in the PLA injection molding or extrusion processes to obtain nanocomposites or coatings [13,17,19,23], with no reports on PLA composites by evaporation-precipitation to produce homogenous coatings over cellulose based paper.

One of the main drawbacks of PLA as coating is its low thermal stability [24]. For instance, reinforcement is required to assure its functional properties by the addition of fillers or other structural modifications. Additionally, its incorporation could cheapen the composite making its manufacturing comparable with low cost polymers. Recently, many reports have assessed the use of nanoscale silicates to improve the structural and barrier properties of PLA films as packaging material. Hectorite, saponite, sepiolite [23] and montomorillonite (MMT) [25] are the main nanoclays employed for this purpose. These nanoclays at low content (<5 wt%), play an important role as fillers into the bio-polymeric matrix [17]; they modify the mechanical, thermal and gas barrier properties as well as the fire resistance of the composite [26]. Natural nanoclay is hydrophilic, so that in order to integrate it into the hydrophobic polymer, an organically-modification is applied [27].

Cloisite$^®$ 30B (CB) is one of the clays more used as an additive for plastics and rubbers. It has been assessed for reinforcement, as flame retardant and as a barrier in the composites [26]. This clay also has been tested together with other biopolymers to enhance the coating surface formation and to give more resistance and better barrier characteristics to the material [15,16,25,28].

Krikorian and Pochan [29] evaluated three commercial organophilic clays (Cloisite 30B, 25A, and 15A). When Cloisite 30B is used as modifier, the better miscibility and reinforcement of the PLA films were attained, due to the interaction between diols and the carbonyl of the PLA backbone. Rhim *et al*. [25], prepared PLA films with the incorporation of three different montmorillonite clays (two modified nanoclays, Cloisite 20A, Cloisite 30B and one unmodified, Cloisite Na$^+$) to improve tensile strength and water vapor permeability (WVP). They found that tensile strength of the films decreased 10%–20% depending on the MMT type. The WVP of nanocomposite films compounded with organically modified nanoclays (20A and 30B) decreased, while the one with Cloisite Na$^+$ (unmodified nanoclay), increased slightly. This was attributed to the hydrophobicity of organically modified nanoclays. In another study, the addition of montmorillonite improved the mechanical properties and the thermal stability of nanocomposites based on polylactic acid and linear low density polyethylene [17].

The effort to produce cellulose based paper for food packaging, coated with PLA to improve its barrier properties and make it competitive with non-biodegradable polymers is still a challenge for research.

Cristallinity depends on the ability of the polymeric chains to pack together to conform an ordered structure. If the polymer presents a relative simple backbone, packing is promoted and a crystalline structure is attained. The order depends on the local organization. When a monomer structure is asymmetric, packing could be diminished and an amorphous material is obtained [30].

In polymers, the interactions presented among the chains are defined by their chemical functionality and the electrostatic forces such as hydrogen bonding. There is always the presence of conformational defects, which alter the crystalline domains into the polymer. Chains can fold back on one another, producing a disordered structure. Polymers do not present fully crystalline structure, for instance they are recognized as semi crystalline [31]. Crystalline and amorphous regions always coexist in a polymer. Crystalline regions could be recognized in different shapes and lengths. Fully amorphous

polymers are characterized by any regular arrangement in a long range, among the molecules. All these factors and their interactions are complicated, affecting the polymer physical properties [32].

Packages are materials, which can be based on polymers, where some structure-sensitive properties are fundamental. In our study, water vapor transmission rate (WVTR), contact angle and grease resistance were the principal properties evaluated. Regarding the difference in structure and morphology found among semi crystalline and amorphous PLA, the principal interest of our work was to study both materials, provided by dissolution on a halogenated solvent, to produce coatings for cellulose paper. Besides, Cloisite 30B was used as filler with the aim to intercalate it into the PLA in such different morphologies.

Thus, the objective of this work is to investigate the effects of montmorillonite, CLA concentration and cristalinity, on PLA-cellulose based coated papers and to evaluate their grease and water barrier properties, in comparison with three commercial packaging papers used in food industry.

2. Experimental Section

2.1. Materials

Two types of polylactic acid (PLA), amorphous (AM, PLA 4060D) and semi crystalline (SC, PLA 2002D) Ingeo Biopolymer, in the form of pellets were supplied by NatureWorks LLC (Minnesota, MN, USA). Chloride methylene (J.T. Baker, Phillipsburg, NJ, USA) was used as solvent. Cellulose paper used as support for PLA coating was kindly supplied by COPAMEX (Chihuahua, México), with a thickness of 60 μm and a grammage of 54.1 g·m^{-2}. Montmorillonite clay, (Cloisite 30B, Southern Clay Products Inc., Gonzales, TX, USA) was used to reinforce the coated-paper. Non-coated paper was used as a control.

As references, three commercial materials (Grease Proof Paper 1, Grease Proof Paper 2, and Glassine Paper) were used for comparative proposes. Glassine paper is a cellulose bleached paper produced by mechanically refining. Grease Proof Papers 1 and 2 are poli-fluorinated coated papers used for food packaging.

2.2. Coating Solutions

Preparation of PLA-based coating solutions was made as described by Rhim *et al*. [25] with some modifications. Five grams of PLA-AM or PLA-SC were dissolved in 100 mL of methylene chloride while mixing at 180 rpm during 1 h at room temperature (23 °C), followed by sonication for 2 h at the same temperature. Moreover, 1% montmorillonite clay Cloisite 30B (CB) solution was prepared in chloride methylene to incorporate it to PLA coating one. The CB solution was mixed with the previously prepared PLA solution and sonicated for 30 min. PLA-montmorillonite clay coating solutions were prepared at 0.1%, 0.25%, 0.5%, 0.75%, 1.0% and 1.5% for each PLA type (AM or SC) with 0, 5 and 10 pph (part clay per 100 parts PLA) of clay (CB).

2.3. Coating Application

Paper packaging was cut into 90 mm of diameter and placed into 90 mm glass petri dishes avoiding wrinkles. Ten milliliters of PLA-montmorillonite clay coating solutions were casted onto packaging paper and allowed to dry at 23 ± 2 °C and 39% ± 4% RH (relative humidity) during 16 h. After drying

all coated papers were peeled from petri dishes and conditioned at 30 °C and 40% HR for at least 48 h before tests.

2.4. Paper Thickness Measurement

Paper thickness was measured at 10 random points using a digital Vernier Mitutoyo (CD-6" CS, Mitutoyo Corp., Tokyo, Japan). Measurements were obtained just after the packages were obtained and conditioned as mentioned in Section 2.3.

2.5. Contact Angle (CA)

Hydrophobicity of coated papers was measured through a Contact angle analyzer FTA 200 (First Ten Amstrongs, Portsmouth, VA, EU). Coated paper samples were cut into 3 cm × 9 cm and fitted on a sample stage and leveled horizontally. A drop of distilled water (10 µL) was placed on the surface of coater paper using a microsyringe. Analyses were carried out at six independent times and the mean ± standard deviation is reported.

2.6. Water Vapor Permeability (WVP)

Water vapor permeability (WVP) was determined gravimetrically according to the ASTM E96 standard method [33]. The method was performed by sealing a paper to an open mouth of a test cup containing silica gel and placing the assembly into a controlled environmental desiccator at 98% ± 2% relative humidity (RH) and 25 °C. The water vapor absorbed by silica gel was detected by weighing the silica containing cup periodically at 1, 2, 4, 6, 8 and 24 h. For each measurement, at least three replications were made. WVP was calculated as:

$$\text{WVP} = \frac{\text{WVTR}}{A}\frac{x}{\Delta P_v} \tag{1}$$

where WVTR is the water vapor transmission rate (g/h), x is the film thickness (µm), A is the transfer area of the exposed film surface (m^2), ΔP_v is partial pressure difference in kPa, respectively.

2.7. Grease Permeability (GP)

Grease resistance of coated, non-coated and reference papers was determined using a modified TAPPI (Technical Association of the Pulp and Paper Industry) test T 454 om−10 [34]. Briefly, the test specimen was placed onto a clean white sheet of paper. Five grams of dry sand were placed into 25 mm iron tube onto the test specimen to obtain a heap and 1.1 mL of red dyed turpentine was added dropwise to the heap of sand. The time in seconds was measured and indicated as the result after which the first turpentine red penetration appears on a white sheet of paper present underneath the test specimen. According to this method, a time of 1800 s corresponds to a high penetration resistance to fats and oils. The time in seconds was reported and the higher grease resistant paper was the specimen with the longer time (1800+).

2.8. Scanning Electron Microscopy (SEM)

Coated paper micrographies were obtained with a Scanning electron microscopy JEOL JSM-5800LV (Tokyo, Japan). The samples were treated in a covering system (Denton Desk-II Gatan, Pleasanton, CA, USA) with gold. SEM photomicrographs were taken at 15 kV in top, bottom and edge views. The structures were analyzed at magnification of 200× and 1000×.

2.9. Confocal Laser Scanning Microscopy (CLSM)

Images of paper coated with PLA-SC 1.5% and 10 pph of montmorillonite were taken with an LSM 700 confocal microscope (Carl Zeiss, Jena, Germany) using the 10×, 20× objectives and the 50× oil immersion objective. Before recording images, PLA-SC/montmorillonite solution was dyed with acid fuchsin (1.0%) and applied over the paper. Once the PLA coated paper was dried, it was dyed with Calcoflour White Stain (18909 Sigma, St. Louis, MO, USA) and let it dry.

2.10. Differential Scanning Calorimetry (DSC)

Differential scanning calorimetry (DSC) analyses were carried out using a TA Instruments calorimeter, DSC-Q 1000, New Castle, DE, USA) under air atmosphere. Samples were heated at a scanning rate of 10 °C·min^{-1} from 30 to 200 °C. The glass transition temperature (T_g) was obtained from the first heating curve. The melting temperature (T_m) and cold crystallization temperature (T_{cc}) were obtained from the second heating curve. The crystallinity degree (X_c) was calculated by using Equation (2), where mf is the weight fraction of PLA in the sample, ΔH_m is the enthalpy of fusion, ΔH_{cc} is the enthalpy of cool crystallization and $\Delta H_m^c m$ is the heat of melting of purely crystalline PLA (93 J·g^{-1}), Lim, [35]:

$$X_c = 100 \times [(\Delta Hm - \Delta Hcc)/\Delta H_m^c m] \frac{1}{1\text{-}mf} \qquad (2)$$

2.11. Gel Permeation Chromatography (GPC)

The molecular weight of the PLA-AM and PLA-SC (pellets) as well as their films in clay absence or at 10 pph, was determined using a gel permeation chromatograph (GPC) Agilent 1100 (Santa Clara, CA, USA), with a ZORBAX bimodal column (Santa Clara, CA, USA). The mobile phase used was tetrahydrofuran (HPLC (High Performance Liquid Chromatography) grade) with a flow rate of 1.0 mL·min^{-1} at 40 °C. Refraction index detector was used for determination. Calibration for GPC technique was made using polystyrene standards of different molecular weight. The samples were prepared at a concentration of 1 mg·mL^{-1} in the same eluent. The composites were re-dissolved from the films, casted into 90 mm glass petri dishes at 23 ± 2 °C and 39% ± 4% HR during 16 h.

2.12. Statistical Analyses

All determinations were carried out at least in triplicate. A full 2 × 6 × 3 factorial design was used with two different PLA, six PLA concentrations and three concentrations of montmorillonite. Data analysis was carried out using Minitab Statistical Software Version 16 (Minitab Inc., State College,

PA, USA). Data were analyzed using an ANOVA (Analysis of Variance) followed by Tukey's multiple-range tests with a 95% of confidence.

3. Results and Discussion

3.1. Scanning Electron Microscopy (SEM) and Confocal Laser Scanning Microscopy (CLSM)

An optical view of all the PLA coatings, before they were casted onto cellulose paper, is presented in Figure 1. All composites evidence homogeneity at every condition. When impregnated to paper, the same behavior was presented. SEM and CLSM evaluation of all the coated materials was made, and selected micrographies are presented here (Figure 2). The surface of the coatings shows a tubular agglomeration through along the material. During the deposition process temperature is below their glass transition temperatures (Section 3.6) leading to a glassy state behavior, which directs the deposition mechanism to a morphological change bound to a possible semi-crystalline growth. For all the composites obtained the same performance was noticed, material presents a tubular pattern throughout the analyzed surface (frontal face) and total adhesion is revealed. This was also reported by Lim [35], who spread PLA onto the surface of cellulose papers and reported also PLA total adherence to the substrate used. The transversal cut only revealed the discontinuities due to the cellulose fibers which forms the base paper.

Figure 1. (**A**) PLA–SC 3%; (**B**) PLA–AM 3%; (**C**) PLA–SC 3% 5 pph; (**D**) PLA–AM 3% 5 pph; (**E**) PLA–SC 3% 10 pph; (**F**) PLA–AM 3% 10 pph; (**G**) PLA–SC 1%; (**H**) PLA–SC 1% 5 pph; (**I**) PLA–AM 1%; and (**J**) PLA–AM 1% 5 pph.
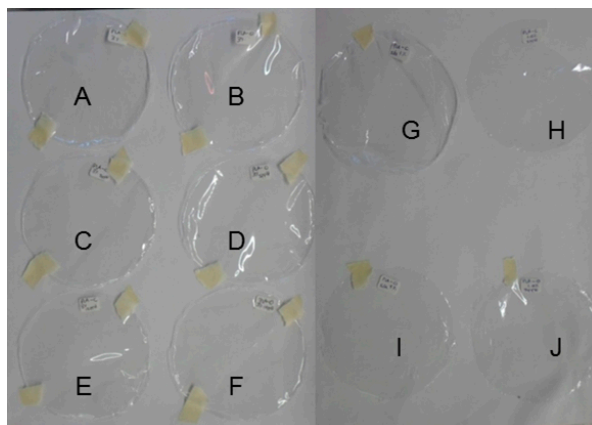

3.2. Paper Thickness Measurement

The thickness is the principal factor that affects the functional properties of a material. The thickness of the different PLA coated, uncoated and reference papers are presented in Table 1. Thickness of uncoated paper was 60 ± 2 μm. This value was not affected by PLA concentration at low concentration (0.1% and 0.25%). Significant differences ($p = 0.000$) were observed from 0.5% to 1.5%. Rhim *et al.* [25] reported an increment in weight and thickness with PLA concentration for PLA-paperboard based packages. They also verified high PLA sealing from 1% PLA. CB concentration did not affected paper thickness ($p = 0.615$).

Table 1. Thickness, CA and grease resistance of coated, uncoated and references papers.

PLA Type	PLA (%)	BC (pph)	Thickness (µm)	CA (°)	GP (seg)
Semicrystalline	0.1	0	59 ± 3	78.9 ± 3.4	583
		5	60 ± 0	76.1 ± 2.9	1800+
		10	61 ± 3	71.9 ± 1.5	900
	0.25	0	60 ± 0	73.9 ± 2.4	1800+
		5	60 ± 0	71.1 ± 5.9	1633
		10	60 ± 0	77.1 ± 3.2	1800+
	0.5	0	68 ± 4	75.0 ± 0.5	1800+
		5	69 ± 3	70.5 ± 1.5	1800+
		10	69 ± 3	73.1 ± 3.5	654
	0.75	0	63 ± 5	74.0 ± 1.4	1800+
		5	64 ± 5	71.3 ± 3.9	270
		10	65 ± 13	74.8 ± 1.2	ND
	1	0	73 ± 7	72.1 ± 2.1	1800+
		5	81 ± 10	71.3 ± 1.2	1452
		10	77 ± 9	73.1 ± 1.6	1282
	1.5	0	72 ± 4	76.4 ± 2.4	1800+
		5	70 ± 5	ND	1800+
		10	72 ± 8	72.3 ± 0.9	ND
Amorphous	0.1	0	58 ± 4	76.6 ± 2.7	1064
		5	56 ± 5	73.2 ± 6.5	1553
		10	58 ± 4	74.6 ± 3.4	360
	0.25	0	60 ± 0	75.2 ± 1.4	1800+
		5	61 ± 6	74.1 ± 2.7	1800+
		10	60 ± 0	73.5 ± 2.2	1800+
	0.5	0	69 ± 7	74.5 ± 2.1	1800+
		5	69 ± 6	74.5 ± 1.6	1800+
		10	73 ± 7	75.3 ± 2.3	1800+
	0.75	0	68 ± 4	73.0 ± 6.4	1800+
		5	68 ± 6	75.1 ± 1.9	1800+
		10	75 ± 14	74.8 ± 3.7	1800+
	1	0	73 ± 7	72.5 ± 3.3	1053
		5	78 ± 8	72.9 ± 2.3	1800+
		10	74 ± 5	73.6 ± 2.2	1800+
	1.5	0	84 ± 18	73.0 ± 2.7	1800+
		5	80 ± 19	73.0 ± 2.6	1800+
		10	74 ± 7	73.8 ± 2.3	1800+
Glassine Paper			40 ± 0	66.1 ± 3.2	95
Grease Proof Paper 1			60 ± 0	65.7 ± 3.5	135
Grease Proof Paper 2			60 ± 0	80.7 ± 2.4	1095
Uncoated paper			60 ± 2	11.9 ± 3.7	2

pph: parts of clay per 100 parts of PLA; CA: Contact angle; ND: Not determined.

Figure 2. SEM (Scanning Electron Microscopy) and confocal micrographies of a film of PLA-SC 1.5% 10 pph: (**a**) Front view, 200×; (**b**) Transversal cut 1000×; and (**c**) Confocal micrography, 1000×.
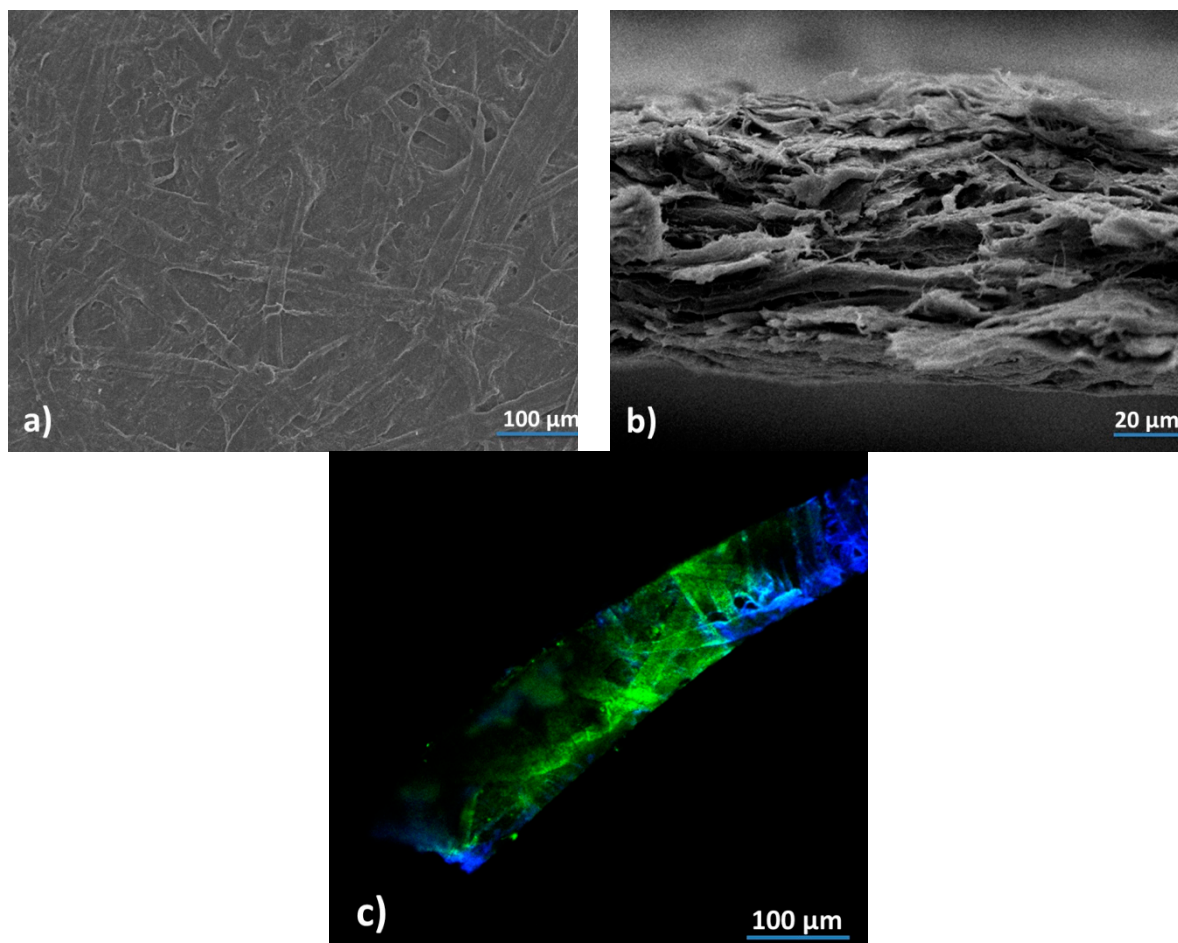
3.3. Contact Angle (CA)

The measurement of water contact angle is used to determinate the hydrophobicity of a sample. It can be correlated with the barrier properties of the coatings obtained [22,36]. The CAs of the materials were measured and results are presented in Table 1. The contact angle varies significantly as a function of PLA concentration ($p = 0.00$) and PLA type ($p = 0.041$). CB loading is not affecting this parameter at each PLA concentration. In all cases studied, PLA-AM contact angles are higher than the ones measured for PLA-SC. PLA concentration, no matter its nature, also increases CA.

CA is determined by the physicochemical nature of the material tested. When polar substances are used, it is plausible to have a partial rearrangement of the functional groups towards the surface during casting. In this case, diols and carbonyls of PLA, evidenced later on by FTIR (Section 3.5), should create a three dimensional network with the cellulose –OH, and the non-polar part of the structure may be reoriented to the air interface, producing the high CA values measured. In the work by Arrieta *et al.*, 2014 [37] paper nanocomposite films based on PLA and poly(hydroxybutyrate) blends and cellulose nanocrystals (CNC) (unmodified and neat) were prepared, and analyzed mechanically, optically, and in their barrier properties towards oxygen and water. Nanocomposites obtained were evaluated as short-term food packaging, thus they additionally studied the disintegration process in composting

conditions. The formulations made with modified CNC (sulfonate functionalized) showed enhanced mechanical properties, water resistance and an appropriate disintegration in compost. For all the formulations evaluated, the contact angle showed values higher than 65°, nevertheless the presence of CNC presented a significant effect in both PLA and PLA–PHB (polylactic acid-hydroxybutyrate) blends. It increased the wettability while CNCs did not significantly modify this parameter. Additionally, for the degradability studies, they reported that PLA–PHB–CNC films presented the highest disintegration rate due to the –OH surface polarity. The orientation of the hydroxyl groups catalyzed the hydrolysis process.

Amorphous PLA present no crystalline domains, as evidenced by DSC (Section 3.6), so partial reorientation may demand less energy than the one with semicrystalline PLA. Rhim *et al.* [38] studied the CA of paperboards coated with 1–5 *w/v*% PLA. The contact angle of paperboards coated with less than 1 *w/v*% PLA was lower than the one of uncoated paperboard then it increased up to 73° when coated with more than 3 *w/v*% of PLA. Generally, the increment in the contact angle of water by PLA coatings indicates a decrease in hydrophilicity of the surface, which is attributed to the hydrophobicity of PLA. Fortunati *et al.* [39], reported contact angle of neat PLA 3051D (M_n of 1.4×10^4 mol·g^{-1}) as 73° ± 2°. When they blended PLA with 20% and 25% of limonene, CA decreased until 54° ± 3° and 51° ± 2° respectively, but when they blend PLA with nanocrystals of cellulose the wettability of polymer was not affected (71° to 74°). They attributed the reduction of the contact angle to limonene plasticization effect. Rhim *et al.* (2006) [40] prepared chitosan composite films with 5 wt% modified Cloisite 30B and Cloisite Na$^+$ (high hydrophilic character). They found a decrease of CA, in 3.2°, when Cloisite 30B was used. They obtained unexpected high CA results when they blend chitosan with cloisite Na$^+$ (47.4°). Moreover, Magalhães and Andrade [41] found the contrary effect on thermoplastic corn starch hybrids with cloisite Na$^+$ and cloisite 30B. CA increased with the incorporation of cloisite 30B.

The increase in CA of cellulose based paper by PLA coating indicates that the water resistance of composites could be improved by PLA coating. These results are consistent with WVP [36]. All materials generated presented a CA value superior to the references used. CA of uncoated paper was 11.99° ± 3.73° meanwhile the references papers ones were 65.71° ± 3.56°, 66.05° ± 3.19° (Grease Proof Paper 1 and Glassine Paper, respectively). For instance, PLA coatings prepared are more hydrophobic than the commercial ones used in terms of their CA.

3.4. Grease Permeability

Grease resistance is important for packaging products containing fats or oils. There are few reports about grease barrier of packaging materials. Plastics may be classified as excellent, good, poor or no barrier to grease. Polyethylene, polypropylene and most plastics are generally classified as good grease barriers [4]. In the same sense, grease barrier properties are required for packaging foods with high grease content such as fast food. In addition, grease permeation through paper packaging affects product appearance.

TAPPI T454 test gives an accelerated comparison of the relative rates at which oils or greases penetrate papers. According to this, a time of 1800 s corresponds to a high penetration resistance to fats and oils [42]. In this study, all composites show a high grease resistance as it can be observed in

Table 1. For PLA–AM all the composites prepared show penetration times of more than 1800, but for low PLA concentration. Grease diffusivity also depends on package thickness. Parris *et al.* [5] coated kraft paper with one single layer and double layer zein and paraffin wax. They found that at higher concentrations of coating, good grease resistance was produced.

3.5. Water Vapor Permeability (WVP)

Water vapor permeability is an important property because it indicates the amount of water that can pass through the packing material, *i.e.*, it can determine the speed at which water molecules can diffuse through the material and its solubility. High WVP can result in faster packaged food deterioration and mechanical problems during handling or storage. Therefore, it is intended that packages, which are in direct contact with high moisture content foods, have low WVP to ensure its stability.

The tendencies of the WVP are shown in Figure 3. For low PLA concentration (less than 0.5%) amorphous PLA presents higher WVP than PLA–SC. This is according with other reports where crystalline PLA presented lower WVTR (water vapor transmission rate) than amorphous PLA [43]. It is also well-known that polymer crystallinity reduces the solubility and permeability of water. Crystallites have very low permeabilities so that they, in effect, reduce the cross-sectional area for diffusion and increase the diffusion path length and may also impose restraints on the mobility of the amorphous phase [44]. Tsuji *et al.* [45], observed a correlation among the degree of crystallinity, (X_c), molecular weight and WVTR. WVTR of PLA films decreased monotonically with increasing X_c from 0% to 20%, and explained this change in terms of the higher resistance of the restricted regions compared to the free ones to water permeation. For comparison, WVTR for other common polymers: polystyrene, 6.4 $g/m^2/day$; polyethylene terephtalate 1.2 $g/m^2/day$; and polypropylene, 0.3 $g/m^2/day$ [46].

WVP is a parameter which depends on hydrophobicity of the composite. When ANOVA is applied for each set of data corresponding to the CB loading variation, no difference is attained ($p = 0.392$). CB is not affecting also this parameter in the condition tested and concentration evaluated.

Molinaro *et al.* [16], studied the corresponding thermo-compressed PLACB films. They reported that the addition of CB affected the WVTR, decreasing significantly ($p < 0.05$). Other studies performed by Rhim *et al.* [25], specified that the WVP of the nanocomposite films decreased 6%–33% through nanoclay compounding. Among the clay types used, Cloisite 20A was the most effective in improving the water vapor barrier. All these cases are for thermo-compressed PLA films with no incorporation to a cellulosic substrate. In our work, solvent casting and paper adhesion process is used to obtain PLA–CB coatings. CB incorporation into the material occurs during evaporation precipitation; thus non-thermal treatment was made. The ultrasonic dispersion could affect clay penetration into the polymeric network. Cloisite as a layered silicate is considered as a continuous stack of clay platelets disposed in a crystalline structure [47]. The clay presents a hydrophilic nature and in most of the cases, the ions are exchanged by cationic organic ones (in our case CB is ammonium modified) to improve their compatibility with polymers [48]. In thermo-compressed films PLA molecular weight is affected by the thermal treatment. Chain reduction could promote clay-polymer interaction. In our case, molecular weight remains almost unaltered after sonication, when PLA was dissolved for film preparation (Table 2). One factor could be correlated to the lack of well

penetration of the CB and PLA during casting. To confirm the clay interaction into the polymeric matrix, FTIR and DSC of the higher loaded films were obtained and presented further (Sections 3.5 and 3.6).

Figure 3. WVP (water vapor permeability) for the whole experimental design. Reference papers are included. Control corresponded to base cellulose paper of the packages.
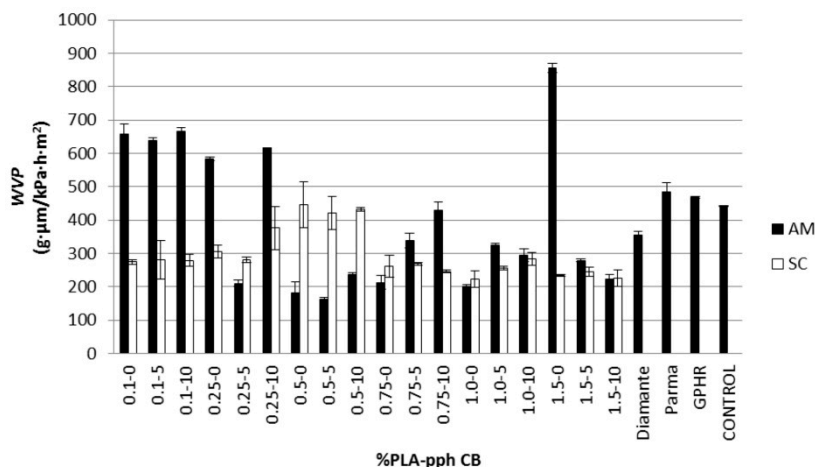
Table 2. DSC /GPC results for PLA–AM and PLA–SC and their films (F).

Parameter/Sample	PLA–AM	PLA–AM (F)	PLA–SC	PLA–SC (F)
T_g (°C)	57.4	56.0	59.0	59.5
T_{cc} (°C)	na	na	132.0	130.0
ΔH crystallization (J·g^{-1})	na	na	3.7	14.0 *
X_c (%)	na	Na	3.1	11.0
M_n (g·mol^{-1})	9.1×10^4	8.14×10^4	1.4×10^5	1.3×10^5
M_w (g·mol^{-1})	2.7×10^5	2.74×10^5	3.3×10^5	3.1×10^5

na: not apply; * clay 10 ppH.

The WVP is not affected significantly neither by PLA nor by its concentration when the last one varies. Other authors reported on paper board that the WVP decreased significantly depending on the PLA concentration. They measured a WVP in the range from $(4.21 \pm 0.27) \times 10^{-9}$ g·mm^{-2}·s^{-1}·Pa^{-1} for the uncoated paperboard, to $(1.31 \pm 0.18) \times 10^{-10}$ g·mm^{-2}·s^{-1}·Pa^{-1} for the 5% PLA-coated paperboard [25]. In the present study, thickness of the composite should play a detrimental role on WVP. For PLA concentration higher than 0.5%, changes in thickness are significant (Section 3.1) thus, the effect on PLA concentration or nature is not observed. This observation is confirmed by the statistical analysis performed which demonstrate positive correlation (0.529) between thickness and WVP (*p* = 0.000). The best WVP obtained in this study was $(4.42 \pm 0.19) \times 10^{-11}$ g·mm^{-2}·s^{-1}·Pa^{-1} for Paper coated with 0.5% PLA–AM and 5 pph of CB, achieving lower values than the reported ones. Finally, uncoated paper did not presented significant differences when compared to Grease Proof Paper 1 and Grease Proof Paper 2.

In water vapor transport, the polymer microstructure is involved. Transport proceeds by a solution-diffusion mechanism. Typically, crystalline PLA regions are not permeable to gases [49]. Crystallites increase tortuosity which affects the diffusion of the penetrants. The effect of a filler is similar than the crystallites regarding diffusion. The area to thickness ratio and orientation of the

additive relative to the permeant direction, affects its diffusivity. In our work, the type of PLA does not attain differences in WVP of the packages, neither the clay. As reported for solution-diffusion mechanisms for barriers, thickness presented a positive correlation with WVP [50]. The possible effect of PLA crystallinity is not evidenced by this parameter but DSC (Section 3.6).

3.6. Fourier Transformed Infrared Spectrometry

Figure 4 shows the IR spectra of PLA–AM and PLA–AM–CB and of the ATR (attenuated total reflectance) of pure cloisite. The Carbonyl group is the most prominent band due to the stretching of the –C=O at 1761 cm^{-1} and carbonyl bending at 1382 cm^{-1}. The –OH stretching band at 3504 cm^{-1} is also characteristic of carboxylic acid [37]. The signals of 2995 and 2945 cm^{-1} correspond to –CH$_2$ and –CH$_3$. The hydroxyl bending is in 1185 cm^{-1}. When Cloisite is added no difference in the infrared pattern is revealed. Pure Cloisite show the band at 3628 cm^{-1} typical to –OH according to the structure reported by the fabricant. Farmahini-Farahani *et al.* [51], found similar FTIR patterns on modified and non-modified Cloisite 30B MMT nanoclay: at 3629 cm^{-1} appeared the –OH stretching, 2924 and 2852 cm^{-1} were attributed to C–H bonds stretching vibrations. In addition, an intense band between 1000 and 1100 cm^{-1} could correspond to Si–O–R group.

Figure 4. FTIR of PLA–AM in **red**, PLA–AM CB (10 pph) in **purple** and pure Cloisite 30B in **Green**.
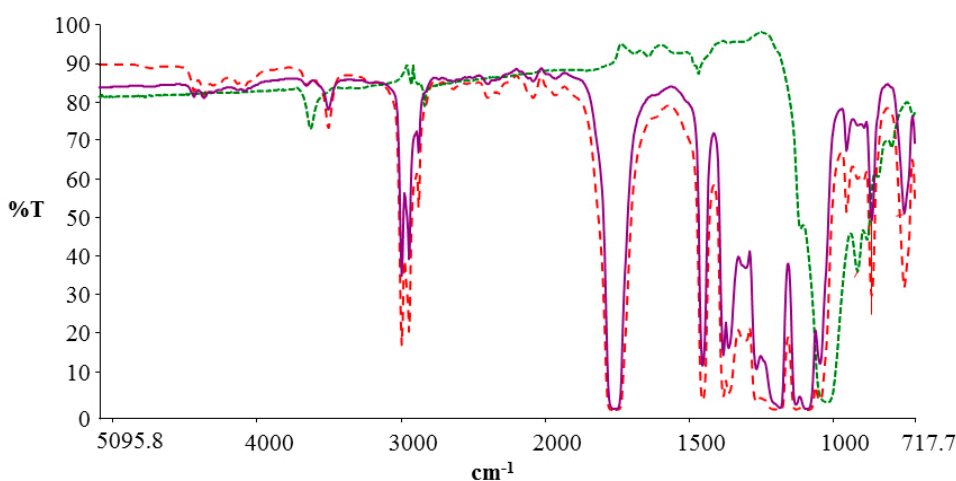
3.7. Differential Scanning Calorimetry (DSC) and Gel Permeation Chromatography (GPC)

Other main properties of polymers are both their thermal characteristics and molecular weight. They influence physicochemical properties such as mechanical (modulus, tensile strength), and transition temperatures (melting point). When filler is used, the thermal events should be modified by the interaction among it and the polymer.

Films of PLA–AM and SC and their composites were studied by DSC. A summary of the thermal events is shown in Table 2. For PLA–SC three thermal events were noticed corresponding to T_g, T_{cc} and T_m; meanwhile for PLA–AM only one, where T_g was obtained. T_g corresponds to the temperature at which the polymer changes from its glassy to a rubbery state and is correlated to the amorphous

region of PLA and the polymer chain mobility. T_m is the temperature that depends strongly on the crystalline regions. T_{cc} is associated to the transition from amorphous to crystalline states.

T_g of the films analyzed change dramatically depending on the PLA and the clay incorporation. It changes for PLA–SC from 57.4 °C to 56 °C when 10% of CB is used. The variation of T_g, by the incorporation of fillers is explained by a plasticizing effect of the PLA polymeric matrix by the organic filler [35,52]. Pluta *et al.* [52], reported a T_g reduction 54.1 °C to 53.2 °C with 3 wt% of montmorillonite. In the case of PLA–SC the difference among its composite is very slight (in 0.5 °C). In the other hand, crystallinity increases from 3.1% to 11%. The crystallinity increases when the filler acts as a nucleation center forming a heterophase which is incorporated to the polymer [53]. Other important factor is polymer molecular weight. For PLA–AM the shorter chains compared to PLA–SC should contribute to the plasticizing effect observed. There is also a non-significant effect of the sonication treatment when the films were obtained. For T_{cc}, it decreases in the PLA–SC–CB. This also was observed by Sinha Ray *et al.* [54], where the T_{cc} of PLA shifted to lower values at high montmorillonite loadings. They suggest that this fact is explained by the nucleation action of the organoclay, contributing to spontaneous crystallization of the PLA. Gårdebjer, S. *et al.* recently reported also an increase in crystallinity of extruded PLA adding microcrystalline cellulose and xyloglucan [55].

4. Conclusions

Polylactic acid in conjuction with CB, as film forming mixture onto cellulose based paper, is a promising polyester bio-based formulation for food packaging. The crystallinity and concentration of PLA were the principal factors that influence the barrier properties of the coating. The contact angles attained for PLA–AM were greater (up to 73°) than the reference commercial papers (Glassine Paper, Grease Proof Papers 1 and 2). The high hydrophobic character of this composite is explained in terms of its physicochemical nature. Its low T_g (57.4 °C) and molecular weight (9.1×10^{-4}), could promote a partial rearrangement of the polymeric chains, promoting the interaction by electrostatic forces among the polar groups of the cellulose and the –OH of PLA. The carbon backbone could be thus exposed to the air interface, promoting better barrier properties than its semi-crystalline counterpart. For grease penetration all materials corresponded to a high penetration resistance to fats and oils according the reference TAPPI test usually used during paper manufacturing. In this property, composites developed show better barrier properties than the commercial grease proof paper.

WVP attained for PLA–AM 0.5% were in the range from 161.36 to 237.8 g·μm·kPa^{-1}·m^{-2}·d^{-1}. These are the lowest values measured. WVP remains constant at PLA concentration higher than 0.25%. This parameter is not affected neither by PLA nature nor by CB, but it is positively correlated with thickness. PLA–SC showed larger WVP for low PLA concentration compared to PLA–AM.

CB loading does not affect significantly the properties analyzed. Nevertheless, clay interaction with the polymer matrix was evidenced by the modification of the thermal properties measured. The three thermal events recognized for PLA–SC were modified at higher values when CB is loaded at the highest concentration used. The Measured ΔH_{crys} of 3.7 J·g^{-1} for PLA–SC and 14 J·g^{-1} for PLA–SC–CB, evidenced clay interaction as a crystal nucleating agent.

Acknowledgments

Author Contributions

Daniela Sánchez Aldana, is the pos-doctoral student whom performed all the packages and the overall experimental work. Eduardo Duarte Villa, research chief of COPAMEX, leads paper development and tests in plant and coordinates this vinculation project with UACH and CIMAV. Miguel De Dios Hernández, the principal research assistant makes all the grease experiments in plant. Guillermo González Sánchez and Sergio Flores Gallardo in CIMAV make all the contact angle and DSC analysis. Quintín Rascón Cruz at UACH makes all GPC analysis. Hilda Piñon Castillo performed the microscopies. Lourdes Ballinas Casarrubias is the leader of the project and makes along Sánchez the whole manuscript and discussion of the results.

Conflicts of Interest

The authors declare no conflict of interest.

References

1. Ham-Pichavant, F.; Sèbe, G.; Pardon, P.; Coma, V. Fat resistance properties of chitosan-based paper packaging for food applications. *Carbohydr. Polym.* **2005**, *61*, 259–265.
2. Begley, T.H.; White, K.; Honigfort, P.; Twaroski, M.L.; Neches, R.; Walker, R.A. Perfluorochemicals: Potential sources of and migration from food packaging. *Food Addit. Contam.* **2005**, *22*, 1023–1031.
3. Yoo, S.; Lau, S.H.; Krochta, J.M. Grease penetration and browning resistance of pulpboard and paperboard coated with whey protein. *Packag. Technol. Sci.* **2012**, *25*, 259–270.
4. Trezza, T.A.; Vergano, P.J. Grease resistance of corn zein coated paper. *J. Food Sci.* **1994**, *59*, 912–915.
5. Parris, N.; Vergano, P.J.; Dickey, L.C.; Cooke, P.H.; Craig, J.C. Enzymatic hydrolysis of zein-wax-coated paper. *J. Agric. Food Chem.* **1998**, *46*, 4056–4059.
6. Zhang, W.; Xiao, H.; Qian, L. Enhanced water vapour barrier and grease resistance of paper bilayer-coated with chitosan and beeswax. *Carbohydr. Polym.* **2014**, *101*, 401–406.
7. Bordenave, N.; Grelier, S.; Coma, V. Hydrophobization and antimicrobial activity of chitosan and paper-based packaging material. *Biomacromolecules* **2009**, *11*, 88–96.
8. Reis, A.B.; Yoshida, C.M.; Reis, A.P.C.; Franco, T.T. Application of chitosan emulsion as a coating on Kraft paper. *Polym. Int.* **2011**, *60*, 963–969.
9. Khwaldia, K. Physical and mechanical properties of hydroxypropyl methylcellulose-coated paper as affected by coating weight and coating composition. *Bioresources* **2013**, *8*, 3438–3452.
10. Hansen, N.M.; Plackett, D. Sustainable films and coatings from hemicelluloses: A review. *Biomacromolecules* **2008**, *9*, 1493–1505.
11. Vink, E.T.; Rabago, K.R.; Glassner, D.A.; Gruber, P.R. Applications of life cycle assessment to NatureWorks™ polylactide (PLA) production. *Polym. Degrad. Stab.* **2003**, *80,* 403–419.

12. Gruber, P.; O'Brien, M. Polylactides "Natureworks® PLA". In *Biopolymers Online*; Wiley-VCH Verlag GmbH & Co. KGaA: Hoboken, NJ, USA, 2002.

13. Fang, Q.; Hanna, M.A. Rheological properties of amorphous and semicrystalline polylactic acid polymers. *Ind. Crops Prod.* **1999**, *10*, 47–53.

14. Petersson, L.; Kvien, I.; Oksman, K. Structure and thermal properties of poly (lactic acid)/cellulose whiskers nanocomposite materials. *Compos. Sci. Technol.* **2007**, *67*, 2535–2544.

15. Svagan, A.J.; Åkesson, A.; Cárdenas, M.; Bulut, S.; Knudsen, J.C.; Risbo, J.; Plackett, D. Transparent films based on PLA and montmorillonite with tunable oxygen barrier properties. *Biomacromolecules* **2012**, *13*, 397–405.

16. Molinaro, S.; Cruz Romero, M.; Boaro, M.; Sensidoni, A.; Lagazio, C.; Morris, M.; Kerry, J. Effect of nanoclay-type and PLA optical purity on the characteristics of PLA-based nanocomposite films. *J. Food Eng.* **2013**, *117*, 113–123.

17. Balakrishnan, H.; Hassan, A.; Wahit, M.U.; Yussuf, A.A.; Razak, S.B.A. Novel toughened polylactic acid nanocomposite: mechanical, thermal and morphological properties. *Mater. Des.* **2010**, *31*, 3289–3298.

18. Hu, R.; Lim, J.K. Fabrication and mechanical properties of completely biodegradable hemp fiber reinforced polylactic acid composites. *J. Compos. Mater.* **2007**, *41*, 1655–1669.

19. Bledzki, A.K.; Jaszkiewicz, A.; Scherzer, D. Mechanical properties of PLA composites with man-made cellulose and abaca fibres. *Compos. A Appl. Sci. Manuf.* **2009**, *40*, 404–412.

20. Fortunati, E.; Armentano, I.; Zhou, Q.; Iannoni, A.; Saino, E.; Visai, L.; Kenny, J.M. Multifunctional bionanocomposite films of poly (lactic acid), cellulose nanocrystals and silver nanoparticles. *Carbohydr. Polym.* **2012**, *87*, 1596–1605.

21. Hughes, J.; Thomas, R.; Byun, Y.; Whiteside, S. Improved flexibility of thermally stable poly-lactic acid (PLA). *Carbohydr. Polym.* **2012**, *88*, 165–172.

22. Arrieta, M.P.; López, J.; Ferrándiz, S.; Peltzer, M.A. Characterization of PLA-limonene blends for food packaging applications. *Polym. Test.* **2013**, *32*, 760–768.

23. Raquez, J.M.; Habibi, Y.; Murariu, M.; Dubois, P. Polylactide (PLA)-based nanocomposites. *Prog. Polym. Sci.* **2013**, *38*, 1504–1542.

24. Kopinke, F.D.; Remmler, M.; Mackenzie, K. Thermal decomposition of biodegradable polyesters—I: Poly (β-hydroxybutyric acid). *Polym. Degrad. Stab.* **1996**, *52*, 25–38.

25. Rhim, J.W.; Hong, S.I.; Ha, C.S. Tensile, water vapor barrier and antimicrobial properties of PLA/nanoclay composite films. *LWT Food Sci. Technol.* **2009**, *42*, 612–617.

26. Sinha Ray, S.; Okamoto, M. Polymer/layered silicate nanocomposites: A review from preparation to processing. *Prog. Polym. Sci.* **2003**, *28*, 1539–1641.

27. Hussain, F.; Hojjati, M.; Okamoto, M.; Gorga, R.E. Review article: Polymer-matrix nanocomposites, processing, manufacturing, and application: An overview. *J. Compos. Mater.* **2006**, *40*, 1511–1575.

28. Carrasco, F.; Gámez Pérez, J.; Santana, O.O.; Maspoch, M.L. Procesado del ácido poliláctico (PLA) y de nanocompuestos PLA/montmorillonita en planta piloto: Estudio de sus cambios estructurales y de su estabilidad térmica. *Afinidad* **2010**, *66*, 14–20. (In Spanish)

29. Krikorian, V.; Pochan, D.J. Poly (L-lactic acid)/layered silicate nanocomposite: Fabrication, characterization, and properties. *Chem. Mater.* **2003**, *15*, 4317–4324.

30. Leephakpreeda, T. Control of Crystallinity Distribution in Polymer Extrusion Process. Ph.D Thesis, The University of Akron, Akron, OH, USA, 1996.

31. Kaur, J.; Lee, J.H.; Shofner, M.L. Influence of polymer matrix crystallinity on nanocomposite morphology and properties. *Polymer* **2011**, *52*, 4337–4344.

32. Kong, Y.; Hay, J.N. The measurement of the crystallinity of polymers by DSC. *Polymer* **2002**, *43*, 3873–3878.

33. ASTM. Standard test methods for water vapor transmission of materials, E 96–80. In *Annual Book of ASTM Standards*; American Society for Testing and Materials: Philadelphia, PA, USA, 1989; pp. 745–754.

34. *TAPPI T 454 om-10 Turpentine test for voids in glassine and greaseproof Papers*; Technical Association of the Pulp & Paper Industry: Peachtree Corners, GA, USA, 2010.

35. Lim, L.T.; Auras, R.; Rubino, M. Processing technologies for poly (lactic acid). *Prog. Polym. Sci.* **2008**, *33*, 820–852.

36. Rhim, J.W.; Kim, J.H. Properties of poly (lactide)-coated paperboard for the use of 1-way paper cup. *J. Food Sci.* **2009**, *74*, E105–E111.

37. Arrieta, M.P.; Fortunati, E.; Dominici, F.; Rayón, E.; López, J.; Kenny, J.M. PLA-PHB/cellulose based films: Mechanical, barrier and disintegration properties. *Polym. Degrad. Stab.* **2014**, *107*, 139–149.

38. Rhim, J.W.; Lee, J.H.; Hong, S.I. Increase in water resistance of paperboard by coating with poly (lactide). *Packag. Technol. Sci.* **2007**, *20*, 393–402.

39. Fortunati, E.; Luzi, F.; Puglia, D.; Dominici, F.; Santulli, C.; Kenny, J.M.; Torre, L. Investigation of thermo-mechanical, chemical and degradative properties of PLA-limonene films reinforced with cellulose nanocrystals extracted from Phormium tenax leaves. *Eur. Polym. J.* **2014**, *56*, 77–91.

40. Rhim, J.W.; Hong, S.I.; Park, H.M.; Ng, P.K. Preparation and characterization of chitosan-based nanocomposite films with antimicrobial activity. *J. Agric. Food Chem.* **2006**, *54*, 5814–5822.

41. Magalhães, N.F.; Andrade, C.T. Thermoplastic corn starch/clay hybrids: Effect of clay type and content on physical properties. *Carbohydr. Polym.* **2009**, *75*, 712–718.

42. Weilbacher, R.; Fuss, R. Process for the Curtain-Coating of Substrates without the Use of Tensides. U.S. Patent 20100112226 A1, 6 May 2010.

43. Shogren, R. Water vapor permeability of biodegradable polymers. *J. Environ. Polym. Degrad.* **1997**, *5*, 91–95.

44. Ashley, R.J. Permeability and plastics packaging. In *Polymer Permeability*; Comyn, J. Ed.; Springer: Dordrecht, The Netherlands, 1985; pp. 269–308.

45. Tsuji, H.; Okino, R.; Daimon, H.; Fujie, K. Water vapor permeability of poly (lactide)s: Effects of molecular characteristics and crystallinity. *J. Appl. Polym. Sci.* **2006**, *99*, 2245–2252.

46. Barrie, J.A. Water in polymers. *In Diffusion in Polymers*; Crank, J., Park, G.S., Eds.; Academic: London, UK, 1968; pp. 259–308.

47. Duncan, T.V. Applications of nanotechnology in food packaging and food safety: Barrier materials, antimicrobials and sensors. *J. Colloid Interface Sci.* **2011**, *363*, 1–24.

48. Pilla, S. *Handbook of Bioplastics and Biocomposites Engineering Applications*; John Wiley & Sons: Hoboken, NJ, USA, 2011.

49. Sato, S.; Nyuui, T.; Matsuba, G.; Nagai, K. Correlation between interlamellar amorphous structure and gas permeability in poly(lactic acid) films. *J. Appl. Polym. Sci.* **2014**, *131*, doi:10.1002/APP.40626.

50. Campbell, D.; Pethrick, R.A.; White, J.R. *Polymer Characterization: Physical Techniques*; Stanley Thornes (Publishers) Ltd.: Cheltenham, UK, 2000; p. 38.

51. Farmahini-Farahani, M.; Xiao, H.; Zhao, Y. Poly lactic acid nanocomposites containing modified nanoclay with synergistic barrier to water vapor for coated paper. *J. Appl. Polym. Sci.* **2014**, *131*, doi:10.1002/APP.40952.

52. Pluta, M.; Galeski, A.; Alexandre, M.; Paul, M.A.; Dubois, P. Polylactide/montmorillonite nanocomposites and microcomposites prepared by melt blending: Structure and some physical properties. *J. Appl. Polym. Sci.* **2002**, *86*, 1497–1506.

53. Sanchez-Garcia, M.D.; Lagaron, J.M. Novel clay-based nanobiocomposites of biopolyesters with synergistic barrier to UV light, gas, and vapour. *J. Appl. Polym. Sci.* **2010**, *118*, 188–199.

54. Sinha Ray, S.; Maiti, P.; Okamoto, M.; Yamada, K.; Ueda, K. New polylactide/layered silicate nanocomposites. 1. Preparation, characterization, and properties. *Macromolecules* **2002**, *35*, 3104–3110.

55. Gårdebjer, S.; Larsson, A.; Lofgren, C.; Strom, A. Controlling water permeability of composite films of polylactide acid, cellulose, and xyloglucan. *J. Appl. Polym. Sci.* **2014**, doi:10.1002/APP.41219.